International Journal of Thermal Sciences 100 (2016) 1–9

Contents lists available at ScienceDirect

International Journal of Thermal Sciences

journal homepage: www.elsevier.com/locate/ijts

The measurements of electrical and thermal conductivity variations with temperature and phonon component of the thermal conductivity in Sn–Cd–Sb, Sn–In–Cu, Sn–Ag–Bi and Sn–Bi–Zn alloys

Yemliha Altıntas [a], Yusuf Kaygısız [b], Esra Öztürk [c], Sezen Aksöz [d], Kâzım Keşlioğlu [e, *], Necmettin Maraşlı [f]

[a] Abdullah Gül University, Department of Materials Science and Nanotechnology, 38039 Kayseri, Turkey
[b] Necmettin Erbakan University, Department of Energy Systems Engineering, 42310 Konya, Turkey
[c] Kocaeli University, Department of Physics, 41380 Kocaeli, Turkey
[d] Nevşehir Hacı Bektaş Veli University, Department of Physics, 50300 Nevşehir, Turkey
[e] Erciyes University, Department of Physics, 38039 Kayseri, Turkey
[f] Yıldız Technical University, Department of Metallurgical and Materials Engineering, 34210 İstanbul, Turkey

ARTICLE INFO

Article history:
Received 29 April 2015
Received in revised form
2 September 2015
Accepted 4 September 2015
Available online 5 November 2015

Keywords:
Metals and alloys
Phonons
Thermoelectric
thermal analysis

ABSTRACT

The electrical and thermal conductivity variations with temperature for lead-free ternary solders, namely Sn-41.39 at.% Cd-6.69 at.% Sb, Sn-49 at.% In-1 at.% Cu, Sn-50 at.% Ag-10 at.% Bi and Sn-32 at.% Bi-3 at.% Zn alloys, were measured by the d.c. four-point probe method and radial heat flow apparatus, respectively. The contributions of electrons and phonons to the thermal conductivity were separately determined by using the measured values of the thermal and electrical conductivities obtained by the Wiedemann–Franz law in the lead-free ternary solders. The percentages of the phonon component of thermal conductivity were found to be in the range of 46–55%, 46–50%, 38–47% and 69–73% for Sn-41.39 at.% Cd-6.69 at.% Sb, Sn-49 at.% In-1 at.% Cu, Sn-50 at.% Ag-10 at.% Bi and Sn-32 at.% Bi-3 at.% Zn alloys at the ranges of 318–443 K temperature, respectively. The temperature coefficients (α) of electrical conductivity for the lead-free ternary solders were found to be 2.47×10^{-3}, 4.97×10^{-3}, 1.14×10^{-3} and 1.00×10^{-3} K^{-1}, respectively. The thermal conductivities of the solid phases at their melting temperature and the thermal temperature coefficients for the lead-free ternary solders were also found to be 47.72 ± 2.38, 68.57 ± 3.42, 73.52 ± 3.67, 37.53 ± 1.87 W/Km and 1.47×10^{-3}, 1.48×10^{-3}, 1.85×10^{-3} and 2.21×10^{-3} K^{-1}, respectively.

1. Introduction

Investigations of the thermal and electrical properties of alloys are important for many technological applications. In order to characterize and to test the performance and the stability of metallic alloys, electrical and thermal conductivities are essential physical quantities. In the literature, there is not much knowledge about the thermal and electrical properties of lead-free ternary solders. Thus, determining the thermal and electrical properties for lead-free ternary solders could be of great use to researchers and engineers [1].

Heat is carried by electrons, phonons, magnetic excitations, and sometimes photons in solids. The total thermal conductivity is the sum of the thermal conductivities of all energy carriers in a solid. The thermal conductivity of energy carriers can be shown as

$$K_{thermal} = \frac{1}{3} \sum_{j} C_j \, v_j \, l_j \quad (1)$$

where the subscript j demonstrates the kind of carriers. C_j is the the specific heat per unit volume, v_j is the velocity of the carrier and l_j is a mean free path.

Since the electrons and phonons in conductors are the main carriers of heat, the total thermal conductivity of the metal can be expressed as the sum of electron and phonon contributions.

* Corresponding author. Tel.: +90 352 207 66 66x33128; fax: +90 352 437 49 33.
E-mail address: kesli@erciyes.edu.tr (K. Keşlioğlu).

http://dx.doi.org/10.1016/j.ijthermalsci.2015.09.004
1290-0729/

$$K_{thermal} = K_e + K_{ph} \quad (2)$$

where K_e and K_{ph} are the contribution of electrons and phonons to the thermal conductivity, respectively [1].

In metals, which energy carriers transmit the most heat? The contribution of electrons is greater than that of phonons at all temperatures in pure metals. However in disordered alloys or in impure metals, the phonon contribution approaches the electronic contribution owing to the reducing of the electron mean free path [2]. The ratio of the electronic contribution of the thermal conductivity (K_e) to the electrical conductivity (σ) of a metal is expressed as the Wiedemann–Franz law, and this value is proportional to the temperature (T).

$$\frac{K_e}{\sigma} = LT \quad (3)$$

Theoretically, the proportionality constant L, known as the Lorenz number [2], is equal to

$$L = \frac{K}{\sigma T} = \frac{\pi^2}{3}\left(\frac{k_B}{e}\right)^2 = 2.44 \times 10^{-8} W\Omega K^{-2} \quad (4)$$

As can be seen from Eqs. (2) and (3), the contribution of the electron or phonon components to the thermal conductivity can be individually determined from Eqs. (2) and (3) if the electrical conductivity and thermal conductivity of the materials are measured or known at a given temperature.

The main aim of the present work was to determine the phonon component of the thermal conductivity in ternary alloys. To do this, the variations of electrical and thermal conductivities with temperature in the lead-free ternary solders were measured by the four-point probe method and the radial heat flow method, respectively. By using the measured electrical conductivity (σ) value of the alloy, the electronic component of the thermal conductivity (K_e) can be calculated from the Wiedemann–Franz law for a given temperature. Then the phonon component of the thermal conductivity (K_{ph}) can be obtained from Eq. (2) by using the values of calculated K_e and measured $K_{thermal}$.

In the present study, Sn–Cd–Sb, Sn–In–Cu, Sn–Ag–Bi and Sn–Bi–Zn ternary alloys were chosen for measuring the electrical and thermal conductivities. What was the reason for choosing these ternary alloy systems? Since lead and lead-containing materials are very toxic and hazardous for the human body and the environment, the EU Directives on Waste Electrical and Electronic Equipment (WEEE) have forbidden the use of lead in selected electronic devices sold in the European market [3]. Consequently investigation of the properties of lead-free solders is crucial. A number of studies have also been focused on Sn based multicomponent alloys because tin is a reasonably cheap material compared to other alloying elements.

Sn–Sb solder, which contains a low amount of antimony, has good mechanical properties such as creep resistance and mechanical strength [4,5]. Cd has several unique and remarkable characteristics such as excellent resistance to corrosion, good electrical conductance, low melting point, and resistance to chemicals [6]. Therefore the Sn–Cd–Sb ternary alloy can be used in electronic applications because of its low cost, low melting temperature and wettability.

In general, materials which form solder alloys should have lower melting temperatures. Since indium has a low melting temperature it is usually preferred in solder applications. Thus the Sn–In–Cu ternary alloy system is a suitable candidate for lead–tin solders [7].

The Sn–Zn eutectic alloy is a good alternative for a lead-free solder alloy due to its low melting temperature (198 °C), perfect mechanical properties, low cost [8,9] and being harmless to human health and the environment. The Sn–Zn alloy can be used in electronic packaging but it is sensitive to oxidation and corrosion [10–12]. Sn–Bi–Zn and Sn–Bi–Ag which both contain Bi, are good candidates for lead-free solder alloys because these alloys have a low melting temperature and good wettability [13–17].

Thus, the first step of this work is to experimentally measure the variations of electrical and thermal conductivities with the temperature by the four-point probe and radial heat flow methods, respectively in Sn–Cd–Sb, Sn–In–Cu, Sn–Ag–Bi and Sn–Bi–Zn lead-free solders. The second step of the present work is to determine the phonon component of thermal conductivity for the same alloys.

2. Experimental procedure

2.1. Sample production

Sn-41.39 at.% Cd-6.69 at.% Sb, Sn-49 at.% In-1 at.% Cu, Sn-50 at.% Ag-10 at.% Bi and Sn-32 at.% Bi-3 at.% Zn were melted in a vacuum furnace. The purity of all the metals used in the preparation of alloys in the present work was more than 99.9%. After stirring, the molten metal was poured into a graphite crucible in a hot filling furnace. Two different graphite crucibles were used for the experimental measurement of electrical and thermal conductivity. For electrical conductivity measurements, the crucibles were prepared from graphite and were 20 mm in length and 4 mm in diameter. For thermal conductivity measurement, the crucibles were prepared from graphite and were approximately 100 mm in length and 30 mm in diameter. The molten material in the graphite crucible was then directionally solidified from the bottom to the top. More details of the apparatus and experimental procedures are given in Refs. [18,19].

2.2. Measurement of electrical conductivity variation with temperature

Electrical conductivity is an imperative physical property. Impurities deform the lattice in metals and can affect the properties of electrical conductivity/resistivity. The value of electrical conductivity is also affected by grain size, plastic deformation, heat treatment, and some other factors, but to a smaller extent compared to the effect of temperature and chemical composition [20].

Atoms vibrate at all temperatures in the balance positions and the amplitude of the vibrations increases by increasing the temperature of the sample. When the atoms leave from their lattice, vacancies occur in the crystal structure [21]. If the dislocation density increases in the crystal lattice, the possibility of deviation in the electron waves increases, phonon–phonon, electron–electron and phonon–electron inelastic collisions increase, the mean free path decreases, resistance increases and electrical conductivity decreases. These defects may be dislocations, in the corners of the blank lattice, grain boundaries, and substituted atoms [22]. These mechanisms, which depend on composition and temperature, can decrease the electrical conductivity. In metals, electrical conductivity decreases with increasing temperature. The temperature dependency of electrical conductivity can be expressed as

$$\sigma(T) = \sigma_0[1 + \alpha(T - T_0)] \quad (5)$$

where, α is the temperature coefficient of electrical conductivity, T_0 is a fixed reference temperature (usually room temperature), and σ_0 is the conductivity at temperature T_0. Then we can obtain the temperature coefficient of electrical conductivity α from Eq. (5).

$$\alpha = \frac{\sigma - \sigma_0}{\sigma_0(T - T_0)} = \frac{1}{\sigma_0}\frac{\Delta\sigma}{\Delta T} \quad (6)$$

In this study, the dependence of electrical conductivity on temperature in alloy systems was measured by the four-point probe method which is the most commonly used measurement technique. The advantage of the four-point probe measurement technique is that it eliminates the measurement errors owing to resistance. The resistivity of material can be stated as

$$\rho = RCF\frac{V_{measured}}{I_{measured}} \quad (7)$$

where RCF is the resistivity correction factor. RCF depends on the test structure size, the material thickness, the electrodes, size and the position of the electrodes [23]. The current (I) is measured with the two outer probes, and the voltage (V) is measured via the two inner probes.

A four-point probe measurement is made by applying four electrical probes to the specimen. The two of the connection-contacts are used to measure the current flowing through the sample and the other two are used to measure the potential difference between any two points. The constant current and the potential difference on the sample was measured by a *Keithley 2400* source meter and a *Keithley 2700* multimeter, respectively as shown in Fig. 1. Platinum probes were used to measure the current and potential. The temperature of the specimen was measured by using a K-type thermocouple with a diameter of 0.5 mm in a *Nabertherm* type *P320* furnace. The dimensions of the cylindrical sample were 20 mm in length and 2 mm in radius. There are some experimental difficulties during the electrical resistivity measurement. The most difficult part of resistivity measurement is often making a good electrical contact. For a good contact, the surface of the samples was made flat by grinding and polishing, and then thoroughly cleaned with alcohol. Secondly, the measurement system should be calibrated before measuring electrical current and potential. For this purpose, the resistivity measurement system was calibrated for each time for every single alloy system. Finally to increase the measurement sensitivity, the measurements were made at least ten times for each sample. In the present work, the temperature dependence of the electrical resistivity was determined for all ternary alloys in the range of 300 K–442 K by the four-point probe method. Then the electrical conductivity was calculated for all alloys by taking the inverse of the measured the electrical resistivity in the present work.

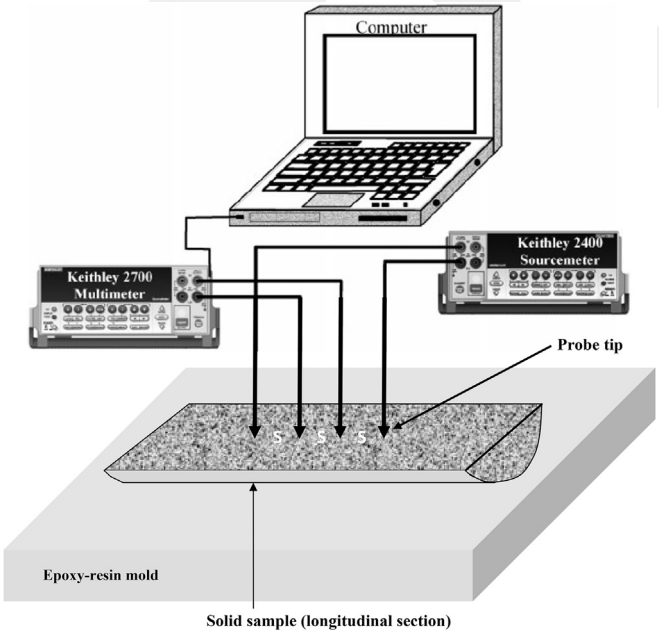

Fig. 1. The schematic diagram of four-probe method used for measuring electrical resistivity/conductivity measurements.

2.3. Temperature dependence of thermal conductivity

In the present work, radial heat flow apparatus have been used to measure the thermal conductivity of the solid phases. The radial heat flow apparatus consists of a central heating wire and a cooling jacket. The central heating wire was at the center of the cylindrical specimen and insulated from materials with a thin walled alumina tube. To get radial heat flow, the specimen was heated from the center using a single heating wire in steps of 50 K up to 10 K below the melting temperature of the alloy and the outside of the specimen was kept cool by circulating a fluid through the cooling jacket. To obtain a reliable value of thermal conductivity in the thermal conductivity measurement, a larger radial temperature gradient is desired. For this purpose, the gap between the cooling jacket and the specimen was filled with free running sand or graphite dust and the outside of the specimen was kept at 283 K using a heating/refrigerating circulating bath. A *Eurotherm 2604* type controller was used to control the temperature of the specimen with an accuracy of ±0.01 K and the temperature of the fluid in the cooling jacket was kept at a constant temperature by a *Poly Science digital 9102* model circulating system. The length of central heating wire was chosen to be 10 mm longer than the length of specimen to make isotherms parallel to the vertical axis. The vertical temperature for each setting was tried to be made as parallel as possible to the vertical axis by moving the central heater up and down.

Consider a cylindrical specimen heated by using a heating wire along the axis at the center of the sample. The temperature gradient of the solid phase at the steady-state condition, is given by Fourier's law

$$G_S = \left(\frac{dT}{dr}\right)_S = -\frac{Q}{A\,K_S} \quad (8)$$

where Q is the total electrical power on the sample, A is the area of the sample and K_S is the thermal conductivity of the solid phase. Integration of Eq. (8) gives

$$K_S = a_o\frac{Q}{T_1 - T_2} \quad (9)$$

where $a_o = \ln(r_2/r_1)/2\pi\ell$ is an experimental constant, ℓ is the length of the central heating wire and T_1 and T_2 are the temperatures at r_1 and r_2 ($r_2 > r_1$). In order to determine the values of K, one has to measure the values of Q, r_1, r_2, ℓ, T_1 and T_2 accurately. One can find the details of the measurement system and procedure in Refs. [18,19,24–29].

The temperature of the sample was kept at a constant temperature for at least 2 h for every measurement. At steady state, a *Hewlett Packard 34401* type multimeter and a data-logger were used to measure the total electrical power and the fixed thermocouples' temperature, respectively. The temperatures of the sample were measured by K-type thermocouples which were 0.5 mm in diameter. The determination of the thermal conductivity was made both in the heating and cooling steps in order to verify the measurement data. In order to determine the thermocouples' positions,

we used an *Olympus DP12 CCD* digital camera connected to an *Olympus BX51* type light optical microscope.

The variation of the thermal conductivity of the solid phase with temperature can be stated as

$$K_S = K_{S0}[1 + \alpha(T - T_0)] \tag{10}$$

where K_S is the thermal conductivity of the solid phase at the temperature T, K_{S0} is the thermal conductivity at the reference temperature T_0 and α is the thermal temperature coefficient. From Eq. (10), α is expressed as

$$\alpha = \frac{K_S - K_{S0}}{K_{S0}(T - T_0)} = \frac{1}{K_{S0}} \frac{\Delta K}{\Delta T} \tag{11}$$

This means that α can be determined from the graph of thermal conductivity with temperature.

3. Results and discussions

3.1. The variation of electrical conductivity with temperature

The variations of electrical conductivity with temperature are plotted in Fig. 2 for Sn–Cd–Sb, Sn–In–Cu, Sn–Ag–Bi and Sn–Bi–Zn solder alloys. The electrical conductivities of all solder alloys in the present work decreased linearly with increasing temperature. The electrical conductivity values as a function of temperature were found in the ranges 4.35–2.76, 5.00–3.43, 5.30–4.58 and 1.52–1.39 ($\times 10^6$)/Ω m for Sn–Cd–Sb, Sn–In–Cu, Sn–Ag–Bi and Sn–Bi–Zn solder alloys, respectively.

The measured electrical conductivity values for solder alloys were compared with the values for the metals forming the alloys [30–34], as shown in Fig. 2. The lines σ for Sn–Cd–Sb, Sn–Ag–Bi and Sn–Bi–Zn solder alloys are extended between those for pure alloying elements, as shown in Fig. 2(a),(c),(d). Since bismuth and antimony are semimetals, their electrical conductivities are very low compared with other metals. Therefore, the electrical conductivities of Sn–Cd–Sb, Sn–Ag–Bi and Sn–Bi–Zn ternary alloys are higher than the electrical conductivities of Bi and Sb. However, the line σ for Sn–In–Cu solder alloy is extended under for Sn, In and Cu, as shown in Fig. 2(b), because all the metals forming the Sn–In–Cu solder alloy individually have good electrical conductivity.

The values of electrical conductivity for Sn–Cd–Sb, Sn–In–Cu, Sn–Ag–Bi and Sn–Bi–Zn at their melting temperatures were obtained as 2.61, 3.26, 4.57 and 1.35 ($\times 10^6$)/Ω m, respectively by extrapolating the electrical conductivity lines to their melting temperature, as shown in Fig. 2.

The temperature coefficients of electrical conductivity were also found to be 2.47×10^{-3} K^{-1}, 4.97×10^{-3} K^{-1}, 1.14×10^{-3} K^{-1} and 1.00×10^{-3} K^{-1} from the graphs of electrical conductivity versus temperature for Sn–Cd–Sb, Sn–In–Cu, Sn–Ag–Bi and Sn–Bi–Zn solder alloys, respectively.

3.2. The variation of thermal conductivity with temperature

The experimental data used in the determination of the thermal conductivities of the solid phases for Sn-41.39 at.% Cd-6.69 at.% Sb, Sn-49 at.% In-1 at.% Cu, Sn-50 at.% Ag-10 at.% Bi, Sn-32 at.% Bi-3 at.%

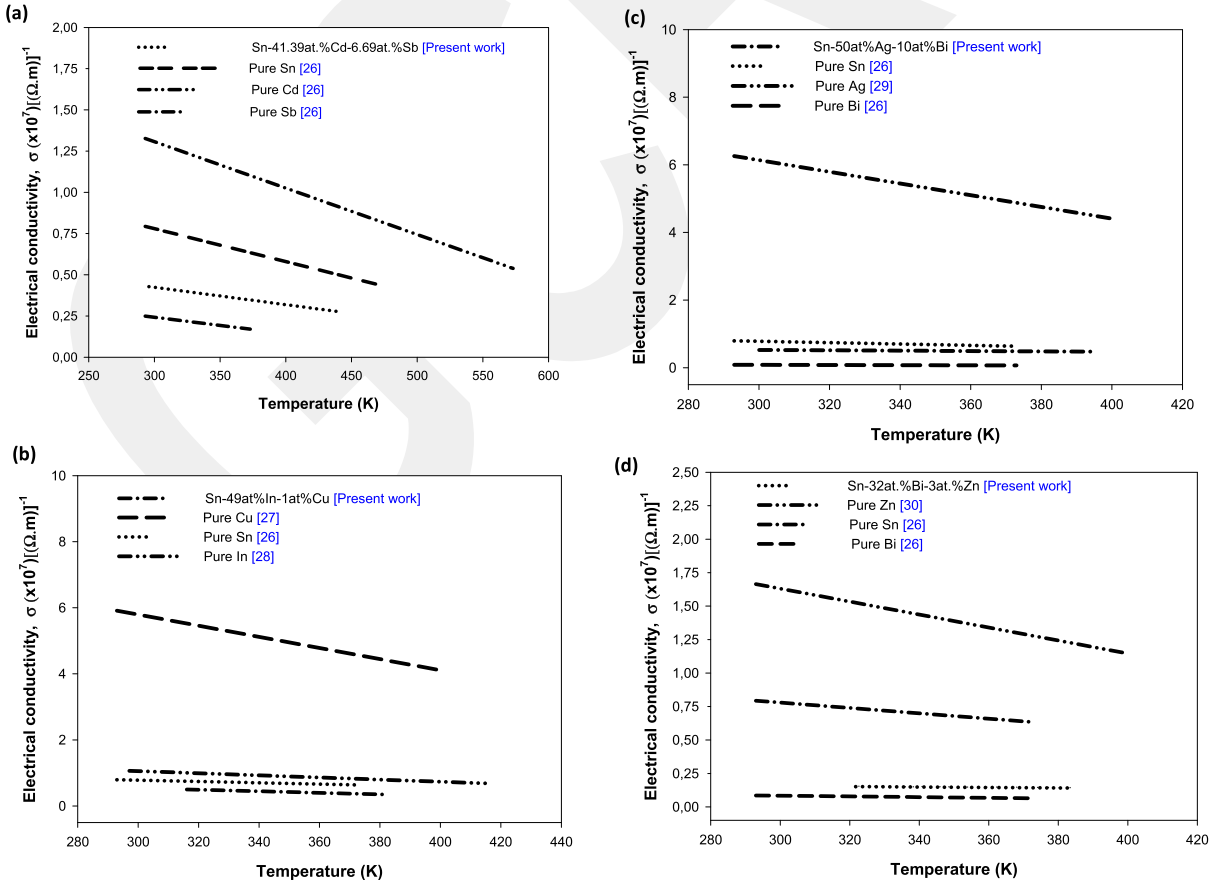

Fig. 2. Temperature dependence of the electrical conductivity for (a) Sn-41.39 at.% Cd-6.69 at.% Sb, (b) Sn-49 at.% In-1 at.% Cu, (c) Sn-50 at.% Ag-10 at.% Bi and (d) Sn-32 at.% Bi-3 at.% Zn solder alloys.

Table 1
Experimental data in the measurements of thermal conductivity variations with temperature for Sn-41.39 at.% Cd-6.69 at.% Sb, Sn-49 at.% In-1 at.% Cu, Sn-50 at.% Ag-10 at.% Bi, Sn-32 at.% Bi-2.99 at.% Zn solder alloys.

T (K)	Sn-41.39 at.% Cd-6.69 at.% Sb			T (K)	Sn-49 at.% In-1 at.% Cu			T (K)	Sn-50 at.% Ag-10 at.% Bi			T (K)	Sn-32 at.% Bi-2.99 at.% Zn		
	Q (W)	ΔT (K)	K (W/Km)		Q (W)	ΔT (K)	K (W/Km)		Q (W)	ΔT (K)	K (W/Km)		Q (W)	ΔT (K)	K (W/Km)
323	17.66	0.52	59.12	318	26.76	0.60	76.14	313	13.90	0.22	92.47	313	22.26	0.70	47.87
353	32.21	0.98	57.38	333	37.21	0.84	75.71	333	22.58	0.38	86.94	333	33.06	1.10	45.24
383	49.24	1.55	55.14	348	47.41	1.10	73.80	353	31.86	0.57	81.79	353	45.34	1.59	42.93
413	67.19	2.27	51.45	363	58.24	1.40	71.32	373	42.51	0.77	80.79	373	58.57	2.12	41.59
443	101.33	3.62	48.71	378	69.76	1.75	68.59	393	52.01	0.99	76.89	393	73.27	2.87	38.71

T: Temperature, Q: Heat flow rate into specimen, ΔT: Temperature difference into specimen, K: Thermal conductivity of specimen.

Zn are given in Table 1. The variations of solid phase thermal conductivity versus temperature for the same alloy systems are also plotted in Fig. 3. As can be seen from Fig. 3, the values of thermal conductivity (K_S) linearly decrease with increasing temperature. The total number of phonons is always proportional to the temperature. Therefore at the temperatures bigger than θ_D (where θ_D is the Debye temperature), the more will be the phonon scattering frequency, resulting in smaller mean free paths. Since C_V approaches the constant Dulong–Petit value, the change in the thermal conductivity is predominantly controlled by the change in mean free path. Thus, the thermal conductivity decreases with increase in temperature [36].

The solubility of solid Cd in Sb and Sn is negligible and 1.1 wt.% Cd at eutectic temperatures of 718 and 406 K, the solubility of solid Sb in Cd and Sn is negligible and 9.6 wt.% Sb at eutectic temperatures of 563 and 515 K, the solubility of solid Sn in Cd and Sb is negligible with 43.6 wt.% Sn at eutectic temperatures of 406 and 515 K [37]. The volume fraction of the solid Sn solution is higher than for the other phases below the eutectic temperature in the Sn-41.39 at.% Cd-6.69 at.% Sb alloy. As shown

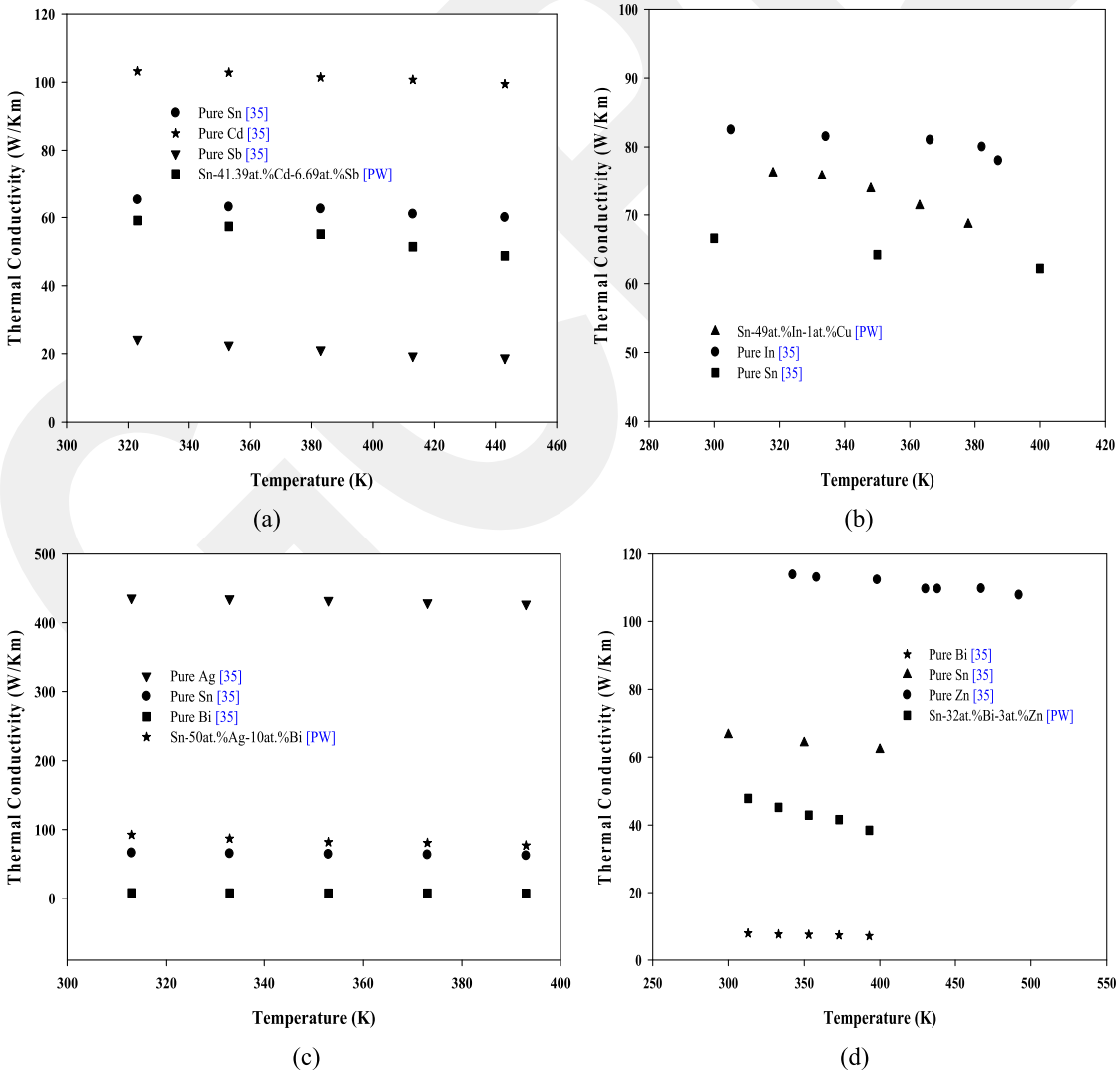

Fig. 3. Thermal conductivity variations with temperature for (a) Sn-41.39 at.% Cd-6.69 at.% Sb, (b) Sn-49 at.% In-1 at.% Cu, (c) Sn-50 at.% Ag-10 at.% Bi, (d) Sn-32 at.% Bi-3 at.% Zn.

in Fig. 3, the thermal conductivity variation for the Sn-41.39 at.% Cd-6.69 at.% Sb alloy is just below the thermal conductivity value for Sn [35].

The solubility of the solid Cu in Sn and In is negligible at eutectic temperatures of 500 and 430 K, the solubility of solid In in Sn and Cu is 27.0 and 18.1 wt.% In at eutectic temperatures of 393 and 847 K, the solubility of solid Sn in Cu and In is 11 and 44.8 wt.% Sn at eutectic temperatures of 623 and 393 K [37]. The volume fraction of solid Sn is close to the volume fraction of the In solution below the eutectic temperature in the Sn-49 at.% In-1 at.% Cu alloy. As shown in Fig. 3, the thermal conductivity variation for the Sn-49 at.% In-1 at.% Cu alloy lies between the thermal conductivity lines of Sn [35] and In [35].

According to the phase diagrams of the Sn–Ag, Sn–Bi and Bi–Ag binary systems, the solubility of solid Ag in Sn and Bi is negligible at eutectic temperatures of 494 and 535 K, the solubility of solid Bi in Sn and Ag is 20 and 2 wt. % Bi at eutectic temperatures of 412 and 535 K, and solubility of solid Sn in solids of Ag and Bi is 27 wt.% Sn and negligible at eutectic temperatures of 494 and 412 K [37]. The volume fraction of solid Ag in the Sn-50 at.% Ag-10 at.% Bi alloy is higher than for the other solid phases below the eutectic melting temperature. As shown in Fig. 3, the thermal conductivity variation for the Sn-50 at.% Ag-10 at.% Bi alloy lies between the thermal conductivity lines of Sn [35] and Ag [35] and is close to the thermal conductivity line of Sn [35].

The solubility of solid Zn in solids of Sn and Bi is negligible and 2.7 wt.% Zn at eutectic temperatures of 471.5 and 527.5 K, the solubility of solid Bi in Sn and Zn is 21 wt.% Bi and negligible at eutectic temperatures of 412 and 527.5 K, the solubility of solid Sn in Zn and Bi is negligible at eutectic temperatures of 471.5 and 412 K [37]. The volume fraction of the solid Sn solution is higher than for the other phases below the eutectic temperature in the Sn-32 at.% Bi-3 at.% Zn alloy. As shown in Fig. 3, the thermal conductivity line for Sn-32 at.% Bi-3 at.% Zn alloy lies between the thermal conductivity lines of Sn [35] and Bi [35] and is close to the thermal conductivity line of Sn [35].

As can be seen in Table 2, the K_S values for Sn-41.39 at.% Cd-6.69 at.% Sb, Sn-49 at.% In-1 at.% Cu, Sn-50 at.% Ag-10 at.% Bi, Sn-32 at.% Bi-3 at.% Zn at their melting temperatures were obtained as 47.72 ± 2.38, 68.57 ± 3.42, 73.52 ± 3.67 and 37.53 ± 1.87 W/Km, respectively via extrapolating the line of thermal conductivity to their melting temperature. A comparison of the K_S values measured in the present work at their melting temperature for Sn-41.39 at.% Cd-6.69 at.% Sb, Sn-49 at.% In-1 at.% Cu, Sn-50 at.% Ag-10 at.% Bi and Sn-32 at.% Bi-3 at.% Zn with the K_S values for similar ternary eutectic alloys measured in previous works [38–42] is also given in Table 2. As can be seen from Table 2, the results are in good agreement with the results obtained in previous works for similar ternary alloys [38–42].

3.3. The variation of electron and phonon components of the thermal conductivity with temperature

In metals and alloys, the main carriers of heat are electrons and phonons, so the total thermal conductivity is shown as the sum of the contributions of the electrons and phonons. As mentioned above, the thermal and electrical conductivities of the alloys ($K_{thermal}$ and σ) were measured by the radial heat flow and four point probe methods, respectively. The electronic components of thermal conductivity, K_e, for the lead-free ternary alloys were determined from the Wiedemann–Franz law by using the measured values of $K_{thermal}$ and σ at a given temperature. Then the phonon components of thermal conductivity, K_{phonon}, for the lead-free ternary alloys were obtained by subtracting the electronic component of thermal conductivity from the measured thermal conductivity ($K_{thermal}$) at a given temperature. The data used in the determination of temperature dependence of the phonon and electron components of the thermal conductivity for the Sn-41.39 at.% Cd-6.69 at.% Sb, Sn-49 at.% In-1 at.% Cu, Sn-50 at.% Ag-10 at.% Bi, Sn-32 at.% Bi-3 at.% Zn ternary alloys are given in Table 3. The variations of electron and phonon components of thermal conductivity versus temperature for the same solders are also plotted in Fig. 4.

As can be seen from Table 3 and Fig. 4, the values of K_e do not change precisely with temperature and seem to be constant. The experimental results support the Wiedemann–Franz law. According to the Wiedemann–Franz law, the electronic component of thermal conductivity (K_e) is proportional to the product of electrical conductivity with temperature. However, the electrical conductivity linearly decreases with increasing temperature. Thus, according to the Wiedemann–Franz law, the electronic component of thermal conductivity should not change precisely with temperature.

As can be seen from Figs. 3 and 4, the measured values of thermal conductivity of the solid phase ($K_{thermal}$) linearly decrease with increasing temperature and the phonon component of thermal conductivity (K_{phonon}) also linearly decreases with increasing temperature.

As can be seen from Fig. 4(a) and (b), the lines of variation of the electronic component of thermal conductivity with temperature are slightly above those of the phonon component of thermal conductivity with temperature for Sn-41.39 at.% Cd-6.69 at.% Sb and Sn-49 at.% In-1 at.% Cu alloys.

In Fig. 4(c), while the line of variation of the electronic component of the thermal conductivity with temperature is below that of

Table 2
Some electrical and thermal properties of solid phase for Sn-41.39 at.% Cd-6.69 at.% Sb, Sn-49 at.% In-1 at.% Cu, Sn-50 at.% Ag-10 at.% Bi, Sn-32 at.% Bi-3 at.% Zn.

Materials	Melting temperature (K)	Temperature coefficient of electrical conductivity α (K^{-1}) × 10^{-3}	Temperature coefficient of thermal conductivity α (K^{-1}) × 10^{-3}	Electrical conductivity at the melting temperature σ (1/Ω m) × 10^{6}	Thermal conductivity at the melting temperature K (W/Km)
Sn-41.39 at.% Cd-6.69 at.% Sb [PW]	453	2.47	1.47	2.61	47.72
Sn-49 at.% In-1 at.% Cu [PW]	389	4.97	1.48	3.26	68.57
Sn-50 at.% Ag-10 at.% Bi [PW]	411.4	1.14	1.85	4.57	73.52
Sn-32 at.% Bi-3 at.% Zn [PW]	404.7	1.00	2.21	1.35	37.53
Sn-4 wt.% Ag-2 wt.% In Ref. [38]	490.7	–	0.280	–	62.50
Sn-20 wt.% Ag-2 wt.% In Ref. [39]	490.7	–	0.620	–	55.10
Sn-40 wt.% Ag-% 2 wt. In Ref. [39]	490.7	–	0.750	–	49.50
Sn-20 wt.% In-25 wt.% Ag [40]	490.7	–	0.805	–	65.10
Sn-20 wt.% In –10 wt.% Ag [40]	490.7	–	0.867	–	68.10
Sn-20 wt.% In-15 wt.% Ag [41]	486.0	–	0.940	–	55.72
Sn-6 wt.% Sb-5 wt.% Ag [42]	507.8	–	1.246	–	41.96
Sn-42.8 wt.% Bi-0.04 wt.% Cu [42]	411.8	–	2.638	–	20.03
Sn-3.5 wt.% Ag –0.9 wt.% Cu [42]	490.2	–	0.907	–	49.89

Table 3
The temperature dependence of the electron and phonon components to the thermal conductivity for Sn-41.39 at.% Cd-6.69 at.% Sb, Sn-49 at.% In-1 at.% Cu, Sn-50 at.% Ag-10 at.% Bi, Sn-32 at.% Bi-3 at.% Zn solder alloys.

Sn-41.39 at.% Cd-6.69 at.% Sb				Sn-49 at.% In-1 at.% Cu				Sn-50 at.% Ag-10 at.% Bi				Sn-32 at.% Bi-3 at.% Zn			
T (K)	K_e (W/Km)	K_p (W/Km)	$K_{thermal}$ (W/Km)	T (K)	K_e (W/Km)	K_p (W/Km)	$K_{thermal}$ (W/Km)	T (K)	K_e (W/Km)	K_p (W/Km)	$K_{thermal}$ (W/Km)	T (K)	K_e (W/Km)	K_p (W/Km)	$K_{thermal}$ (W/Km)
323	31.69	27.43	59.12	318	38.96	37.18	76.14	313	39.64	52.83	92.47	313	–	–	47.88
353	31.47	25.91	57.38	333	38.89	36.82	75.71	333	40.45	46.50	86.95	333	12.19	33.06	45.25
383	31.38	23.76	55.14	348	38.21	35.60	73.81	353	39.84	41.96	81.80	353	12.66	30.28	42.94
413	32.09	19.36	51.45	363	37.87	33.45	71.32	373	40.41	40.39	80.79	373	13.19	28.41	41.59
443	30.56	18.16	48.71	378	37.93	30.66	68.59	393	40.54	36.36	76.90	393	–	–	38.43

the phonon component of the thermal conductivity with temperature up to 370 K, the line of variation of the electronic component of the thermal conductivity with temperature is above that of the phonon component of the thermal conductivity with temperature above 370 K for the Sn-50 at.% Ag-10 at.% Bi alloy.

According to Fig. 4(d), the line of variation of the phonon component of thermal conductivity with temperature is a little above that of the electronic component of thermal conductivity with temperature for the Sn-32 at.% Bi-3 at.% Zn alloy. The reason for the diminishing electronic component contribution to thermal conductivity for Sn-50 at.% Ag-10 at.% Bi and Sn-32 at.% Bi-3 at.% Zn alloys is due to the presence of bismuth in the alloys. Bismuth is a semimetal and its number of free electrons is smaller than that of the other metals in the alloys. Thus, the higher the bismuth content may be responsible for the higher phonon contribution to thermal conductivity.

4. Conclusions

The variations of electrical and thermal conductivities with temperature for the lead-free ternary solders were investigated. According to the experimental results, the electrical conductivity of

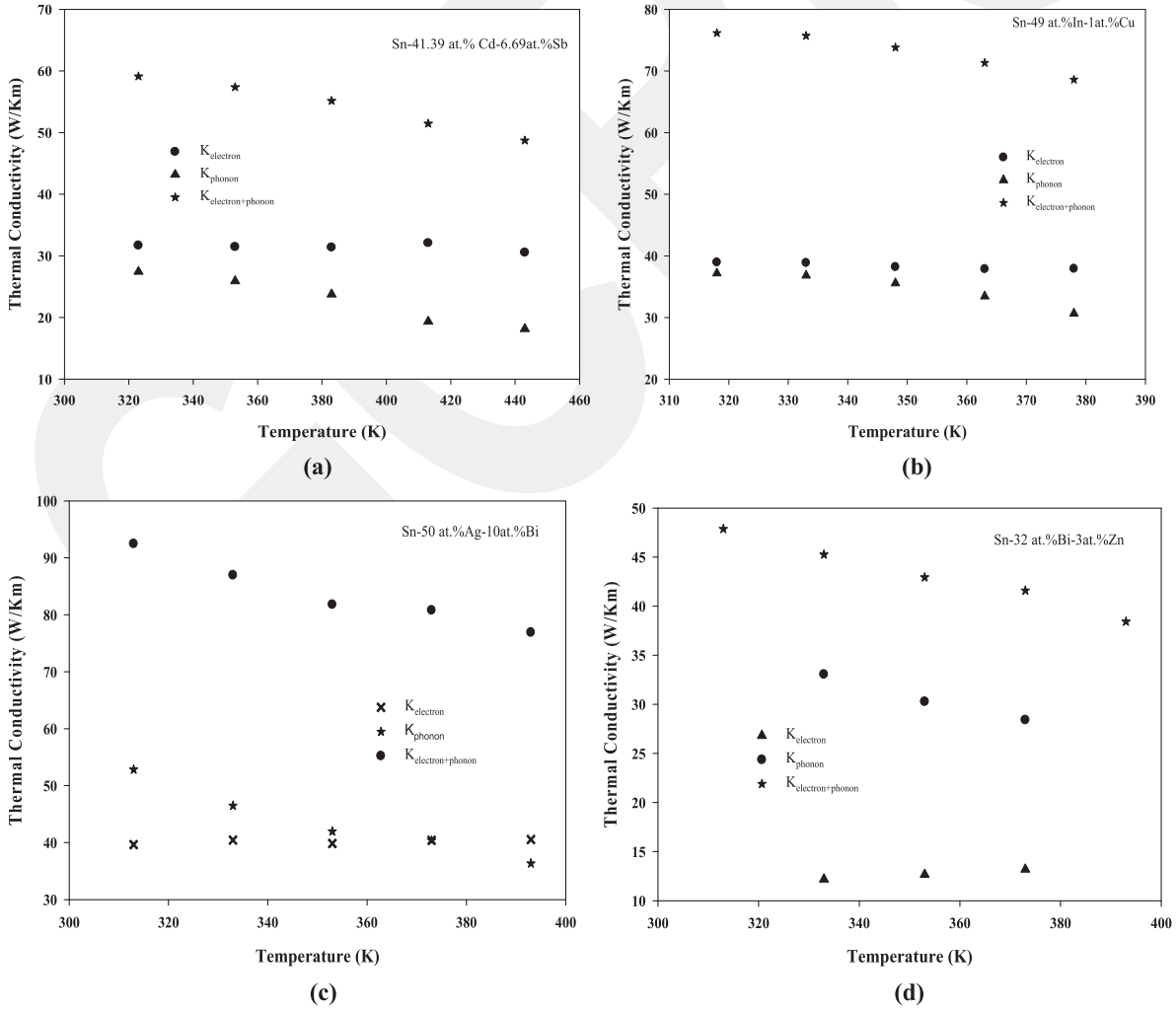

Fig. 4. The temperature dependence of the phonon and electron contribution to the thermal conductivity for (a) Sn-41.39 at.% Cd-6.69 at.% Sb, (b) Sn-49 at.% In-1 at.% Cu, (c) Sn-50 at.% Ag-10 at.% Bi, (d) Sn-32 at.% Bi-3 at.% Zn solder alloys.

the lead-free ternary solders decreases linearly with increasing temperature. Electrical conductivity strongly depends on the temperature and alloying elements used in ternary solders. The values of electrical conductivity for the Sn–Cd–Sb, Sn–In–Cu, Sn–Ag–Bi and Sn–Bi–Zn alloys were obtained as 2.61, 3.26, 4.57 and 1.35 $(\times 10^6)/\Omega$ m, respectively, at their melting temperatures. The temperature coefficients of electrical conductivity for Sn-41.39 at.% Cd-6.69 at.% Sb, Sn-49 at.% In-1 at.% Cu, Sn-50 at.% Ag-10 at.% Bi, Sn-32 at.% Bi-3 at.% Zn solders were determined as 2.47×10^{-3} K^{-1}, 4.97×10^{-3} K^{-1}, 1.14×10^{-3} K^{-1} and 1.00×10^{-3} K^{-1} from the graphs of electrical conductivity versus temperature, respectively.

The thermal conductivity of the lead-free ternary solders also decreases linearly with increasing temperature. The K_S values for the Sn-41.39 at.% Cd-6.69 at.% Sb, Sn-49 at.% In-1 at.% Cu, Sn-50 at.% Ag-10 at.% Bi, Sn-32 at.% Bi-3 at.% Zn alloys were obtained as 47.72 ± 2.38, 68.57 ± 3.42, 73.52 ± 3.67 and 37.53 ± 1.87 W/Km, respectively, at their melting temperature and the temperature coefficients of thermal conductivity for Sn-41.39 at.% Cd-6.69 at.% Sb, Sn-49 at.% In-1 at.% Cu, Sn-50 at.% Ag-10 at.% Bi, Sn-32 at.% Bi-3 at.% Zn were determined as 1.47×10^{-3}, 1.48×10^{-3}, 1.85×10^{-3} and 2.21×10^{-3} K^{-1}, respectively.

Electronic and phonon components of the thermal conductivity for some binary solders were determined before [43] but for ternary alloy systems there isn't enough work. So in this work, electronic and phonon components of the thermal conductivity for some ternary alloy systems were obtained by the Wiedemann–-Franz law by using the measured values of $K_{thermal}$ and σ. From the experimental results it can be concluded that the values of the electronic component of thermal conductivity for the lead-free ternary solders seem to be constant while those of the phonon components of the thermal conductivity for the lead-free ternary solders decrease linearly with increasing temperature. This means that the electronic component of thermal conductivity for pure materials is dominant at all temperatures because the electron mean free path is longer. However, in alloys the phonon contribution approaches the electronic contribution because the mean free path is reduced by collisions with impurities. The percentages of the phonon component of thermal conductivity were found to be in the range of 46–55%, 46–50%, 38–47% and 69–73% for the Sn-41.39 at.% Cd-6.69 at.% Sb, Sn-49 at.% In-1 at.% Cu, Sn-50 at.% Ag-10 at.% Bi and Sn-32 at.% Bi-3 at.% Zn alloys at the temperature range of 318–443 K, respectively.

Ho et al. [43] have determined the phonon components of the thermal conductivity for Cu-x at.%Ni (x = 20, 30, 40, 50, 60, 70, 80) at 300 K. They have determined the total thermal conductivity and the phonon components of the thermal conductivity in the range of 37–33 W/Km and 28%–40% at 300 K, respectively. The phonon components of the thermal conductivity measured in present work are slightly bigger than the values of Ref. [43]. According to phase diagram of Copper and Nickel system [37], solid copper and solid nickel is completely soluble into each other and a single solid phase which has a single crystal structure exists in the Cu–Ni binary system. In present work, at least two phases exist into each alloy system under the melting points. Thus each solid phase contributes to phonon effect on the thermal conductivity. Therefore, the phonon contribution to thermal conductivity for each solid phase must be considered. Thus the phonon contributions obtained in present work are higher than the phonon contribution for Cu–Ni alloy system obtained by Ho et al. [43] due to existed solid phases.

Acknowledgment

This project was supported by the Erciyes University Research Foundation under Contract No: FBA-2013-4746 and by the Nevşehir Hacı Bektaş Veli University Research Foundation under Contract No: NEÜADP13F15. The authors would like to thank Erciyes University and Nevşehir Hacı Bektaş Veli University Research Foundations for their financial support.

References

[1] Y.S. Touloukian, R.W. Powell, C.Y. Ho, P.G. Klemens, Thermal Conductivity Metallic Elements and Alloys, vol. 1, 1970, p. 17a. New York-Washington.
[2] C. Kittel, Introduction to Solid State Physics, sixth ed., John Wiley and Sons, New York, 1965.
[3] J. Vizdal, M.H. Braga, A. Kroupa, K.W. Richter, D. Soares, L.F. Malheiros, J. Ferreira, Thermodynamic assessment of the Bi–Sn–Zn system, Calphad 31 (2007) 438–448.
[4] S. Chen, P. Chen, C. Wang, Melting point lowering of the Sn–Sb alloys caused by substrate dissolution, J. Electron. Mater. 35 (11) (2006) 1982–1985.
[5] M.M. El-Bahay, M.E. El-Mossalamy, M. Mahdy, A.A. Bahgat, Study of the mechanical and thermal properties of Sn–5 wt.% Sb solder alloy at two annealing temperatures, Phys. Status Solidi A 198 (1) (2003) 76–90.
[6] http://www.buzzle.com/articles/cadmium-uses.html.
[7] A.D. Popovic, L. Bencze, Mass spectrometric determination of ternary interaction parameters of liquid Cu–In–Sn alloy, Int. J. Mass Spectrom. 257 (1–3) (2006) 41–49.
[8] W. Yang, R.W. Messler Jr., Microstructure evolution of eutectic Sn–Ag solder joints, J. Electron. Mater. 23 (8) (1994) 765–772.
[9] H. Mavoori, J. Chin, S. Vaynman, B. Moran, L. Keer, M.E. Fine, Creep, stress relaxation, and plastic deformation in Sn–Ag and Sn–Zn eutectic solders, J. Electron. Mater. 26 (7) (1997) 783–790.
[10] Y. Chonan, T. Komiyama, J. Onuki, R. Urao, T. Kimura, T. Nagano, Influence of P content in electroless plated Ni–P alloy film on interfacial structures and strength between Sn–Zn solder and plated Au/Ni–P alloy film, Mater. Trans. 43 (8) (2002) 1887–1890.
[11] S.P. Yu, H.J. Lin, M.H. Hon, M.C. Wang, Effects of process parameters on the soldering behavior of the eutectic Sn–Zn solder on Cu substrate, J. Mater. Sci. Mater. Electron. 11 (6) (2000) 461–471.
[12] NCMS, Lead-Free Solder Project Final Report, NCMS Report 0401 RE 96, National Center for Manufacturing Sciences, Michigan, 1997.
[13] M. Abtew, G. Selvaduray, Lead free solders in microelectronics, Mater. Sci. Eng. 27 (2000) 95–141.
[14] P.L. Liu, J.K. Shang, Interfacial embrittlement by bismuth segregation in copper/tin–bismuth Pb-free solder interconnect, J. Mater. Res. 16 (6) (2001) 1651–1659.
[15] C.N. Chiu, C.H. Wang, S.W. Chen, Interfacial reactions in the Sn–Bi/Te couples, J. Electron. Mater. 37 (1) (2008) 40–44.
[16] S.W. Chen, C.H. Wang, S.K. Lin, C.N. Chiu, Phase diagrams of Pb-free solders and their related materials systems, J. Mater. Sci. Mater. Electron. 18 (2007) 19–37.
[17] I. Artaki, A.M. Jackson, P.T. Vianco, Evaluation of lead-free solder joints in electronic assemblies, J. Electron. Mater. 23 (8) (1994) 757–764.
[18] M. Gündüz, J.D. Hunt, The measurement of solid–liquid surface energies in the Al–Cu, Al–Si and Zn–Pb systems, Acta Metall. 33 (9) (1985) 1651–1672.
[19] N. Maraşlı, J.D. Hunt, Solid-liquid surface energies in the Al–$CuAl_2$, Al–$NiAl_3$ and Al–Ti systems, Acta Metall. 44 (1996) 1085–1096.
[20] V. Rudnev, D. Loveless, R. Cook, M. Black, Markel Dekker Inc, New York, 2003, p. 119.
[21] F. Meydaneri, B. Saatçi, M. Ari, Thermo-electrical characterization of lead–cadmium (Pb–Cd) alloys, Int. J. Phys. Sci. 7 (48) (2012) 6210–6221.
[22] K. Onaran, Material Science Technique Publisher, Istanbul, Turkey, 2009.
[23] L.B. Valder, Resistivity measurements on germanium for transistors, Proc. IRE 42 (1954) 420–427.
[24] K. Keşlioğlu, M. Gündüz, H. Kaya, E. Çadırlı, Solid-liquid interfacial energy in the Al–Ti system, Mater. Lett. 58 (2004) 3067–3073.
[25] M. Erol, K. Keşlioğlu, N. Maraşlı, Solid–liquid interfacial energy of the solid Mg_2Zn_{11} phase in equilibrium with Zn–Mg eutectic liquid, J. Phys. Condens. Matter 19 (17) (2007) 176003–176016.
[26] S. Akbulut, Y. Ocak, N. Maraşlı, K. Keşlioğlu, U. Böyük, E. Çadırlı, H. Kaya, Interfacial energy of solid In_2Bi intermetallic phase in equilibrium with in-Bi eutectic liquid at 72 Degrees C Equilibrating temperature, Mater. Charact. 59 (2008) 1101–1110.
[27] S. Akbulut, Y. Ocak, K. Keşlioğlu, N. Maraşlı, Thermal conductivities of solid and liquid phases for Neopentylglycol, aminomethylpropanediol and their binary alloy, J. Phys. Chem. Solids 70 (2009) 72–78.
[28] K. Keşlioğlu, U. Böyük, M. Erol, N. Maraşlı, Experimental determination of solid–liquid interfacial energy for succinonitrile solid solution in equilibrium with the succinonitrile-(D) camphor eutectic liquid, J. Mater. Sci. 41 (2006) 7939–7943.
[29] Y. Altıntas, E. Öztürk, S. Aksöz, K. Keşlioğlu, N. Maraşlı, The experimental determination of interfacial energies for solid Sn in equilibrium with Sn–Mg–Zn liquid, Metals Mater. Int. 21 (2) (2015) 286–294.
[30] W.F. Gale, T.C. Totemeier, Smithells Metals Reference Book, eighth ed, Elsevier Butterworth-Heinemann, The Boulevard, Langford Lane, Kidlington, Oxford, 2004.
[31] R.A. Matula, Electrical resistivity of copper, gold, palladium, and silver, J. Phys. Chem. Ref. Data 8 (4) (1979) 1161–1174.

[32] S.W. Alpheus, The electrical conductivity of indium and thallium, Ohio J. Sci. 16 (6) (1916) 244–247.
[33] R.A. Matula, Electrical resistivity of copper, gold, palladium, and silver, J. Phys. Chem. Ref. Data 8 (4) (1979) 1260.
[34] P.D. Desal, T.K. Chu, H.M. James, C.Y. Ho, Electrical resistivity of selected elements, J. Phys. Chem. Ref. Data 13 (4) (1984) 1089.
[35] Y.S. Touloukian, R.W. Powell, C.Y. Ho, P.G. Klemens, Thermal Conductivity Metallic Elements and Alloys, IFI/Plenum, New York, 1970 pp.17a, 49,149,185,408,498.
[36] J.P. Srivastana, Elements of Solid State Physics, Prentice Hall of Indian, New Delhi, 2011, p. 139.
[37] M. Hansen, Constitution of Binary Alloys, McGraw-Hill, New York, 1958.
[38] Y. Ocak, S. Aksoz, N. Marasli, K. Keslioglu, Thermal conductivity and interfacial energies of solid Sn solution in the Sn–Ag–In ternary alloy, Chem. Phys. Lett. 496 (2010) 263–269.
[39] Y. Ocak, S. Aksoz, N. Marasli, K. Keslioglu, Thermal and electrical conductivity of Sn–Ag–In alloys, J. Non-cryst. Solids 356 (2010) 1795–1801.
[40] S. Aksöz, N. Maraşlı, Thermal and electrical conductivities of silver–indium–tin alloys, J. Phys. Chem. Solids 73 (2012) 902–910.
[41] E. Öztürk, S. Aksöz, K. Keşlioğlu, N. Marasli, The measurement of thermal conductivity variation with temperature for Sn-20 wt.% in based lead-free ternary solders, Thermochim. Acta 554 (2013) 63–70.
[42] N. Aksöz, E. Öztürk, Ü. Bayram, S. Aksöz, S. Kervan, A. Ülgen, N. Maraşlı, Thermal conductivity variation with temperature for lead-free ternary eutectic solders, J. Elect. Mater 42 (2013) 3573–3581.
[43] C.Y. Ho, M.W. Ackerman, K.Y. Wu, S.G. Oh, T.N. Havil, Thermal conductivity of ten selected binary alloy systems, J. Phys. Chem. Ref. Data 7 (3) (1978) 959–1177.